EVALUATION OF THE PHOTOCATALYTIC ACTIVITY OF α-MoO_3 DOPED WITH RARE EARTH ELEMENTS (La , Y) FOR THE REMOVAL OF METHYL RED DYE

M. KASSEM

Department of Chemistry, Atomic Energy Commission of Syria, Damascus, P.O. Box 6091 Syria
cscientific@aec.org.sy

***Abstract*—This study deals with the use of molybdenum trioxide doped with different quantities of lanthanum or yttrium as catalysts in the photocatalytic processes for removing methyl red from aqueous solution. Crystalline structure, surface area, pore volume, and pore diameter, characteristics that may significantly affect the photocatalytic activity of materials, have been studied, during the addition of lanthanum or yttrium to α-MoO_3, using several advanced techniques such as X-ray diffraction, Raman spectrometry, and nitrogen absorption. Diffraction patterns did not show any changes in α-MoO_3 structure when the doping rate was smaller than 0.6. In doping rates, greater than 0.6, new diffraction peaks related to other compounds have been noticed only in the case of L_xMoO_3. The addition of lanthanum or yttrium has increased the surface area of prepared materials, which contribute to enhancing the photcatalytic activity where the degradation rate of methyl red has reached to about 60% in the case of L_xMoO_3 and to 95% in the case of Y_xMoO_3.**

***Keywords*— Photocatalysis; Methyl red; Lanthanum ; Yttrium ; molybdenum trioxide.**

I. INTRODUCTION

Organic pollutants pose a serious threat to the environment and human health.These pollutants can be released by many industries such as textiles, tanning, electronics, pesticides, chemicals as well as medical establishments (Gong *et al*., 2015; Mansoori *et al*., 2008; Qiu *et al*., 2012). Several methods have been applied to remove these pollutants in order to restore clean environmental conditions. However, most of these methods were either too expensive or cause more damage to the environment, so researchers recently resorted to an advanced process based on sunlight called photocatalysis (Li *et al*., 2015; Moura *et al*., 2017; Shivaraju *et al*., 2017). In this process, many semiconductors based on metal oxides have been widely used as photocatalysts.

Most of them were only active in the field of ultraviolet light because of their large band gap. Scientists have therefore recourse to the doping process with some metals or compounds to adjust the band gap of these substances to make them absorb a greater range of light including visible light and therefore improve the photocatalytic properties (Kiriakidis and Binas 2014; Pei *et al*., 2015; Shao *et al*., 2014; Védrine 2017).

Many doping investigations have been carried out using rare earth elements that could contribute to controlling the band gap of the materials through their empty orbits 4f and 5d.

In addition, these elements have the potential to increase the surface area and pore volume, which enhance the absorbance of organic matter during the photocatalytic process (Areerob and Oh 2017; Meng *et al*., 2016; Shi *et al*., 2012; Yao *et al*., 2012).

MoO_3, one of the wide band-gap semiconductors (about 2.9-3.5eV), has been subjected to a different doping actions with metal impurities in order to be used as a catalyst in many photocatalysis applications (Alfonsoa and Moreno 2014; Chen *et al*., 2010; Eftekhari *et al*., 2016; Li *et al*., 2017; Pereira *et al*., 2008).

The objective of this work is to evaluate the photocatalytic degradation of methyl red from aqueous solutions using photocatalysts materials based on molybdenum trioxide (α-MoO_3) doped with different quantities of a rare earth element (Lanthanum or Yttrium).

II. METHODS

A. Materials Preparation

Doped molybdenum trioxide samples M_xMoO_3 (M= La or Y) were prepared using the impregnation method. A fixed quantity of α-MoO_3 powder (orthorhombic crystal system from Merck, Germany) was suspended in aqueous solution of $M(NO_3)_3.6H_2O$ containing different amounts of lanthanum or Yttrium in order to achieve the molar ratios (M/MoO_3 = 0.02, 0.04, 0.06, 0.08, 0.1). The suspension was heated at 80°C with constant stirring for 4 hours. The solid material was then filtered and washed several times with distilled water, then dried at 120°C. The powder was heated at 650°C for 7 h.

B. Characterization Techniques

The changes that can occur for molybdenum oxide, when adding rare earth elements (La or Y), were studied using a class of advanced techniques: XRD model STOE STADI P operated at room temperature using Cu Kα (λ= 0.154049 nm) and a linear PSD detector at 50 kV and 30 mA. All patterns were measured in 2θ between 5 and 90°, with a step size of 0.02°. A Raman spectrometer, (Jobin Yvon, model Labram-800 with 632 nm Helium Neon laser and a liquid-nitrogen Cooled CCD detector), has also been used to explore structural modifications and molecular arrangements during doping process. To estimate the surface area and pore size, a gas sorption analyzer (Quantachrome NOVA 2200) has been used. All measurements were made by the adsorption of nitrogen gas at the liquid nitrogen temperature.

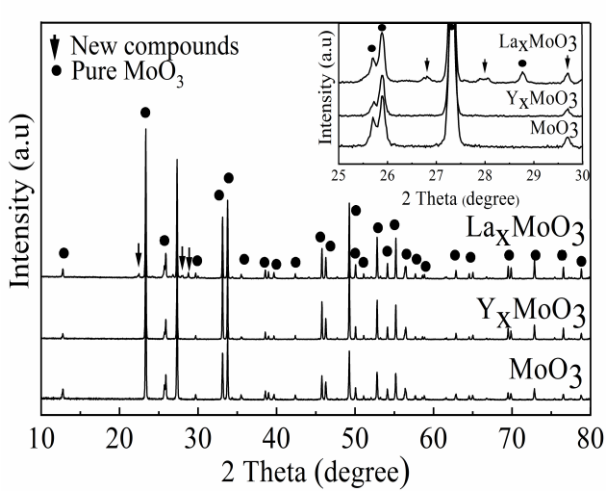

Fig. 1. XRD patterns of pure MoO_3,Y_xMoO_3 and La_xMoO_3 (x= 0.1).

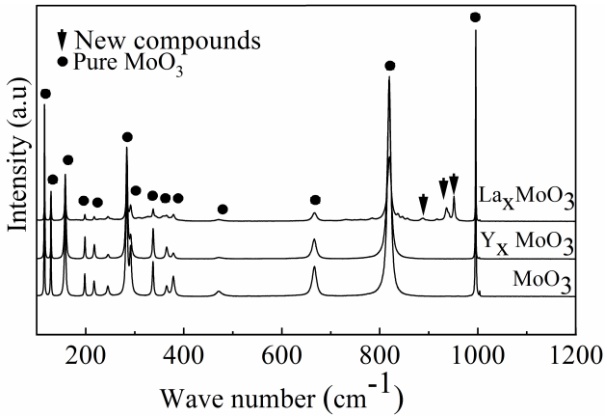

Fig. 2. Raman spectra of pure MoO_3,Y_xMoO_3, and La_xMoO_3 (x= 0.1).

C. Photocatalysis procedure.

For the photocatalysis experiments, 200 mg of the concerned material was suspended in 200 ml methyl red solution (30 mg/l). The suspension has been irradiated, at room temperature with constant stirring, using a commercial 20W UV lamp as a light source. In each run, the concentration of the methyl red was measured three times per hour at λ_{max} = 506 nm, using a UV-spectrophotometer model JENWAY 7415. The degradation rate was calculated using the formula:

$$(\text{Degradation rate } (\%) = [(C_0 - C)/C_0] \times 100$$

where C_0 is the initial concentration of methyl red, C is the concentration at time t .

III. RESULTS AND DISCUSSION

A. Structural and textural analysis

To keep track the structural changes that can occur as a result of the addition of lanthanum and yttrium to α-MoO_3, XRD patterns were collected for all prepared samples. When comparing these patterns, within each set of samples La_xMoO_3 and Y_xMoO_3, no significant changes were detected in molybdenum oxide structure for molar ratios (M/MoO_3, M= La or Y) smaller than 0.06. The comparison was therefore chosen between the XRD patterns for pure orthorhombic α-MoO_3 and samples containing highest molar ratio (M/MoO_3= 0.1) as shown in Fig. 1.

In the case of the La_xMoO_3 group, when the molar ratio increases by more than 0.06, new diffraction peaks begin to appear along with the main peaks of pure molybdenum oxide. These peaks were attributed to the formation of secondary compounds attributed to Mo_8O_{23} (ICDD card N° 84-1248), La_4MoO_9 (ICDD card N° 23-1144) and $La_2Mo_4O_{15}$ (ICDD card N° 23-1146) (Inzani *et al*., 2017; Tokarz-Sobieraj *et al*., 2001). The quantity of these compounds increases with elevation of the molar ratio La/MoO_3. The only significant change , that can be noted in the diffraction patterns of these samples, is the diminution of peaks' intensities related to pure α-MoO_3 (ICDD card N°. 35-609) (Chithambararaj and Chandra Bose, 2011) as a result of the consumption of some of it to form the above mentioned materials. For the Y_xMoO_3 samples group, the related diffraction patterns didn't exhibit any new peaks indicating the formation of additional compounds even at the highest molar ratio (Y/MoO_3=0.1).

The difference in x-ray diffraction results for the two selected groups of samples can be attributed to the difference in physical and chemical properties of both elements lanthanum and yttrium. The atomic radius of the yttrium is smaller than that of the lanthanum, so yttrium can intercalate between the layers of MoO_3 more easily than lanthanum. Moreover, ionization energy for yttrium element is higher than that associated with lanthanum, which makes the latter more reactive. This may be a reason for the formation of additional compounds when adding lanthanum to molybdenum oxide.

With a view to confirm the observations obtained using XRD technique, Raman spectra have been collected for all samples in the both groups La_xMoO_3 and Y_x-MoO_3. In respect of La_xMoO_3 samples, new peaks have been revealed in Raman spectra for the samples containing molar ratios La/MoO_3 greater than 0.06. One can also mention that, in addition to the appearance of these new peaks, there was a decrease in the intensity of the peaks of pure molybdenum oxide (Mihalev, 2014; Sato *et al*., 1986; Zhao *et al*. 2010).

As for the samples of the second group Y_xMoO_3, Raman related spectra did not display any new peaks for all molar ratios Y/MoO_3 from 0 to 0.1. These observations correspond exactly to those obtained using x-ray diffraction. Figure 2 illustrates a comparison between the Raman spectra of pure α-MoO_3, La_xMoO_3 and Y_x-MoO_3 at the highest molar ratio (M/MoO_3 = 0.1).

In the course of specimen characterization procedures, the surface area, pore volume and pore diameter have been measured using nitrogen adsorption technique. These parameters could play an important role in the performance of the material, especially when used as photocatalysts. Table 1 summarizes the values of these parameters for all samples measured according to the above mentioned technique within an error of ± 0.05. By looking through this table, one can observe that the surface area of molybdenum oxide gets larger by

Table 1. Surface area and pore size for pure MoO_3, La_xMoO_3 and Y_xMoO_3 materials ($0<x<0.1$).

Molar Ratio	La_xMoO_3			Y_xMoO_3		
M/MoO_3 (M=La or Y)	Surface area (m^2/g)	Total pore volume (cm^3/g)	Pore diameter (nm)	Surface area (m^2/g)	Total pore volume (cm^3/g)	Pore diameter (nm)
0	0.44	0.80	5.16	0.44	0.80	5.16
0.02	0.49	0.80	5.14	0.50	0.60	4.0
0.04	0.52	0.80	5.06	0.55	0.60	4.0
0.06	0.53	0.70	5.0	0.60	0.60	3.95
0.08	0.55	0.65	4.85	0.65	0.45	3.65
0.1	0.60	0.60	4.0	0.80	0.34	3.0

raising the doping level with both elements (La or Y). However this increment, in surface area, is higher in Y_xMoO_3 group than La_xMoO_3 one. This could be attributed, as suggest earlier, to the soft inclusion of yttrium between α-MoO_3 layers without chemical reaction.

Conversely, for the La_xMoO_3 group, a chemical reaction between lanthanum and molybdenum oxide leads to the formation of secondary compounds that may unfavorably affect the surface area for this type of samples.

B. Photocatalytic activity

The photodegradation of methyl red, in aqueous solutions under ultraviolet light, was selected to evaluate photocatalysis activities for α-MoO_3, La_xMoO_3, and Y_xMoO_3 samples. Through an overview of the results obtained for all of these materials,as shown in Fig. 3, we found that the photocatalytic activity of α-MoO_3 was greatly enhanced by adding elements such as Lanthanum and Yttrium. In either case, the photocatalysis activity is slowly increased for samples with molar ratios M / MoO_3 less than 0.06. By increasing molar ratios to values greater than 0.06, photocatalysis activities of Y_xMoO_3 samples continue to increase until the methyl red degradation rate reaches 95% while not exceeding 60% for La_xMoO_3.

The enhancement in the photocatalytic activity by Lanthanum and Yttrium is generally attributed to the fact that the ions of these elements, through their empty orbits 4f and 5d, work as electronic traps within the bandgap, which reduces the rate of recombination between electrons and holes, generated by UV, and thus promotes the rapid transfer of the electron from the solid to the liquid, and allows holes to interact with the hydroxide ions to form the hydroxide radicals. This is what has been demonstrated through the results of much researches, such as those conducted on TiO_2 (Štengl *et al*., 2009)

Furthermore, the disparity in the photocatalytic activity of the two groups of samples, La_xMoO_3 and Y_xMoO_3, can be attributed to the difference in the phase composition and surface area values, especially at high molar ratios, where it was observed that the doping with lanthanum led to the formation of additional crystalline phases beside of the α-MoO_3 while the yttrium was intercalated inside the layered structure of α-MoO_3 where it can move freely without forming other crystalline

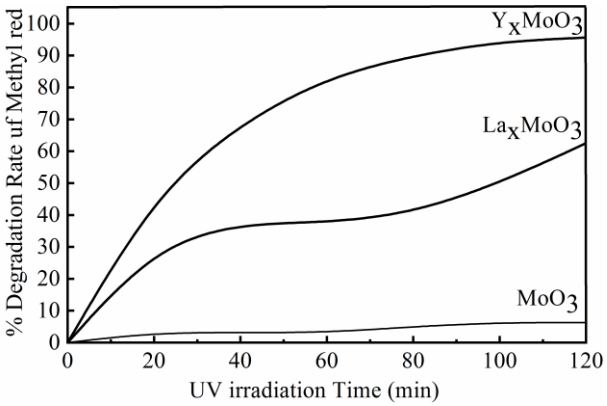

Fig. 3. Photocatalytic degradation rate of methyl red using pure MoO_3, La_xMoO_3 and Y_xMoO_3 (x= 0.1).

phases that could contribute in the reduction of the photodegradation of methyl red.

In addition to the above, the difference in the surface area values for the two series can alter the nature of the contact between the photocatalyst and the methyl red and thus the photocatalytic activity changes.

It is worth noting here that the role of the methyl red absorption process has been excluded through the chemical equilibrium in the dark for two hours before beginning to use ultraviolet radiation.

IV. CONCLUSIONS

The impregnation method was an effective approach for the preparation of photocatalysts based on rare earth metals (La or Y) doped Molybdenum trioxide.

Advanced techniques such as XRD, Raman and nitrogen adsorption were very helpful to track the changes in structural properties, surface area and pore size of molybdenum oxide while adding different amounts of (La or Y). The results obtained using the above mentioned techniques revealed a clear variation in phase composition .This diversity has had a significant impact on the photocatalytic activity, where the degradation rate of methyl red was remarkably changed with the alteration of these properties due to the addition of a rare earth element (La or Y) to molybdenum oxide.

The degradation rate of the methyl red is greatly increased, when the Y_xMoO_3 samples have been used as photocatalysts, to reach more than 95% within 120 minutes while this rate did not exceed 60% when using La_xMoO_3 samples.

ACKNOWLEDGMENTS

The author would like to thank Professor I. Othman, Director General and Dr. Z. Ajji, Head of the Chemistry Department for their encouragement. Thanks are also to Mr. H. Harmalani for assistance in the experimental works as well as Ms. Z. Hariri and Mr. J. Abuhilal for the spectroscopic measurements.

REFERENCES

Alfonsoa, J.E., and Moreno, L.C. (2014) Preparation and chemical characterization of neodymium-doped molybdenum oxide films grown using spray pyrolysis. *Rev. Mex. Fís.* **60**, 114–118.

Areerob, Y., and Oh, W.C. (2017) Enhanced Photocatalytic Properties of Visible Light Responsive La/TiO_2–Graphene Composites for the Removal of Rhodamin B in Water. *J. Korean. Chem. Soc.* **61**, 168-178.

Chen, Y., Lu, C., Xu, L., Ma, Y., Hou, W., and Zhu, J.J. (2010) Single-crystalline orthorhombic molybdenum oxide nanobelts: synthesis and photocatalytic properties. *Cryst. Eng. Commun*. **12**, 3740–3747.

Chithambararaj, A., and Chandra Bose, A. (2011) Hydrothermal synthesis of hexagonal and orthorhombic MoO_3 nanoparticles. *J. Alloys Compd.* **509,** 8105–8110.

Eftekhari, A., Rahmani, M.B., and Masdarolomoor, F. (2016) Effect of Sn Doping on Structural and Optical Properties of 2D α-MoO_3 Nanostructures. *J. Part. Sci. Technol*. **2**, 87-93.

Gong, X., Wang, H., Yang, C., Li, Q., Chen, X., and Hu, J. (2015) Photocatalytic degradation of high ammonia concentration wastewater by TiO_2. *Future. Cities. Environ.*, **1**, 1-12.

Inzani, K., Nematollahi, M., Vullum-Bruer, F., Grande, T., Reenaa, T.W., and Selbach, S.M. (2017) Electronic properties of reduced molybdenum oxides. *Phys. Chem. Chem. Phys*., **19**, 9232-9245.

Kiriakidis, G., and Binas, V. (2014) Metal Oxide Semiconductors as Visible Light Photocatalysts. *J. Korean Phys. Soc*., **65**, 297-302.

Li, W.T., Huang, W.Z., Zhou, H., Yin, H.Y., Zheng, Y.F., and Song, X.C. (2015) Synthesis and photoactivity enhancement of Ba doped Bi_2WO_6 Photocatalyst. *Mater. Res. Bull*. **64**, 432–437.

Li, Z., Wang, W., Zhao, Z., Liu, X., and Song, P. (2017) One-step hydrothermal preparation of Ce-doped MoO_3 nano belts with enhanced gas sensing properties. *RSC. Adv*., **7**, 28366–28372.

Mansoori, G.A., Batami, T.R., Ahmadpour, A., and Eshaghi, Z. (2008) Environmental applications of nanotechnology. *Annu. Rev. Nano. Res*. **2**, 439-493.

Meng, W., Hu, R., Yang, J., Du, Y., Li, J., and Wang, H. (2016) Influence of lanthanum-doping on photocatalytic properties of $BiFeO_3$ for phenol degradation. *Chin. J. Catal*., **37**, 1283–1292.

Mihalev, M.S. (2014) A Comparison between Different Materials Based on Transition Metal Oxides as Additives for Laser Bonding on Stainless Steel. *A.U.J.T.* **18**, 53-56.

Moura, K.F., Chantelle, L., Rosendo, D., Longo, E., and. Santos, I.M.G.d. (2017) Effect of Fe^{3+} Doping in the Photocatalytic Properties of $BaSnO_3$ Perovskite. *Mater. Res*. **120**, 317-324.

Pei, J., Ma, W., Li, R., Li, Y., and Du, H. (2015) Preparation and Photocatalytic Properties of TiO_2-Al_2O_3 Composite Loaded Catalysts. *J. Chem.* **2015**, 1-7.

Pereira, L.G., Soledade, L.E.B., Ferreira, J.M., Lima, S.J.G., Fernandes Jr., V.J., Arájo, A.S., Paskocmas, C.A., Longo, E., Santo, M.R.C., Souza, F.A.G., and Santos, I.M.G. (2008) Influence of doping on the preferential growth of MoO_3. *J. Alloy. Comp*. **49**, 377–385.

Qiu, M., Zhang, J., and Ni, J. (2012) Study on adsorption of Methylene Blue by the Modified Kaolin. *Adv. Mater. Res*. **450**, 60-63.

Sato, M., Fujishita, H., Sato, S., and Hoshino S. (1986) Structural transitions in Mo_8O_{23}. *J. Phys. C: Solid State Phys*. **19,** 3059-3068.

Shao, G.N., Imran, S.M., Jeon, S.J., Engole, M., Abbas, N., Haider, M.S., Kang, S.J., and Kim, H.T. (2014) Sol–gel synthesis of photoactive zirconia–titania from metal salts and investigation of their photocatalytic properties in the photodegradation of methylene blue. *Powder. Technol*. **258**, 99–109.

Shi, Z.L., Lai, H., Yao, S.H. and Wang, S.F. (2012) Preparation, Characterization and Photocatalytic Activity of Lanthanum Doped Mesoporous Titanium Dioxide. *Chin. J. Chem. Phys*. **25**, 96-102.

Shivaraju, H.P., Midhun, G., Anil Kumar, K.M., Pallavi, S., Pallavi, N., and Behzad, S. (2017) Degradation of selected industrial dyes using Mg-doped TiO_2 polyscales under natural sun light as an alternative driving energy. *Appl. Water. Sci*. **7**, 3937–3948.

Štengl, V., Bakardjieva, S., and Murafa, N. (2009) Preparation and photocatalytic activity of rare earth doped TiO_2 nanoparticles. *Mater. Chem. Phys*. **114,** 217–226.

Tokarz-Sobieraj, R., Hermann, K., Witko, M., Blume, A., Mestl, G., and Schlögl, R. (2001) Properties of oxygen sites at the MoO_3(010) surface: Density functional theory cluster studies and photoemission experiments. *Surf. Sci*. **489**, 107-125.

Védrine, J.C. (2017) Heterogeneous Catalysis on Metal Oxides. *Cataly*. **7**, 341-366.

Yao, S., Jia, X., Jiao, L., Zhu, C., and Shi, Z. (2012) La doped hollow fiberd and their photocatalytic activity under UV and Visible light. *Indian. J. Chem. Sect. A*. **51**, 1049-1056.

Zhao, D., Li, F., Yao, Y.M., Huan, C., and Zhao, E.X. (2010) β-$Nd_2Mo_4O_{15}$. *Acta Crystallogr. Sect. E , Struct. Rep*. **66**, i85.

Received: August 21, 2019
Sent to Subject Editor: October 11, 2019
Accepted: October 25 2020
Recommended by Subject Editor Maria Luján Ferreira